New insights into oyster high-resolution hinge growth patterns

Damien Huyghe, Marc de Rafélis, Michel Ropert, Vincent Mouchi, Laurent Emmanuel, Maurice Renard, Franck Lartaud

New insights into oyster high-resolution hinge growth patterns

Damien Huyghe[1,2,3], Marc de Rafelis[2], Michel Ropert[4], Vincent Mouchi[1,5], Laurent Emmanuel[5], Maurice Renard[5], Franck Lartaud[1*]

[1] Sorbonne Université, CNRS, Laboratoire d'Ecogéochimie des Environnements Benthiques, LECOB, F-66650, Banyuls-sur-mer, France

[2] Géosciences Environnement Toulouse, CNRS, IRD, Université Paul Sabatier Toulouse 3, 14 Avenue Edouard Belin, 31400 Toulouse, France

[3] Now at MINES ParisTech, PSL University, Centre de Géosciences, 35 rue St Honoré, 77305 Fontainebleau Cedex, France

[4] Ifremer, Laboratoire Environnement Ressource de Normandie, Avenue du Général de Gaulle, BP 32, 14520 Port-en-Bessin, France

[5] Sorbonne Université, CNRS-INSU, Institut des Sciences de la Terre Paris, ISTeP, F-75005 Paris, France

* corresponding author: F. Lartaud (franck.lartaud@obs-banyuls.fr)

Abstract

While oyster shells are one of the most common mollusks used for the analysis of (paleo)environmental and (paleo)climatic records based on geochemical proxies, high-resolution growth rate changes still need to be determined. Promising previous works are restricted to small portions of shell sections due to difficulties in continuous growth increments revelation. Based on a mark and recapture experiment of *Magallana gigas* specimens reared in an intertidal area of Normandy (France) for 22 months, and a sclerochronological approach using cathodoluminescence microscopy, this study provides the longest high-resolution record of growth increments in oyster shells to date. Different growth patterns were identified likely related to the oyster age. After age one year, the formation of growth increments follows an expected tide-related model, leading to the mineralization of ~2 calcitic increments per day, together with growth rate changes at lunar and semi-lunar periodicities, and a seasonal trend with occasional growth breaks during winter when temperatures fall below ~6 °C. However, for oysters younger than one year, i.e. before reaching their sexual maturity, the growth increments analysis reveals unconventional patterns. In this case, oysters growth is associated with either a large number (~ 5) or less than one increments per day depending on the period. This pattern is also associated with frequent growth cessations, although the growth rate of the shell is high at this period. Our results illustrate that the high-resolution sclerochronological approach is required for accurate paleoenvironmental reconstructions based on oyster shells.

Keywords: sclerochronology, cathodoluminescence, bivalve shells, *Magallana gigas*, paleoclimatology.

Introduction

Bivalves inhabit a variety of different aquatic ecosystems, including freshwater, coastal and deep-sea environments. They produce shell carbonate that both support the general shape of the organisms as well as protect soft tissues against biotic or abiotic threats. However, the shell is not produced consistently over time (Goodwin et al. 2003). Periodic slowdowns of growth, controlled by environmental triggers and/or endogenous mechanisms, result in the formation of growth lines, which separate the growth into regular time intervals of (sub)equal duration, the growth increments (Schöne 2008). This typically results in the formation of annual, lunar, daily or tidal growth increments (Evans 1972; Schöne et al. 2003). The analysis of physical and chemical variations in the shell of organisms, and the temporal context in which they formed is called 'sclerochronology' (Hudson et al. 1976; Gröcke and Gillikin 2008). The sclerochronology of bivalve shells is widely used in ecological and (paleo)environmental studies. Growth increment counting provides a clue to estimating the life span of the organism, as for the 'Methuselah' bivalve *Arctica islandica* reaching 507 years (Butler et al. 2013), together with a potential archive of the organism's environmental conditions (Schöne and Surge 2005). The latter raised a particular interest for shell material from inaccessible habitats (e.g., deep-sea hydrothermal vents, Schöne and Giere 2005; Nedoncelle et al. 2015) or for paleoclimatic reconstructions (Scource et al. 2006; Butler et al. 2013; Schöne 2013). Additional geochemical proxies can also provide a complementary estimation of (past) water conditions, based on the analysis of stable isotopes and trace elements of the shell (Krantz et al. 1987; Dettman et al. 2004; Chauvaud et al. 2005; Ivany et al. 2008; Lartaud et al. 2010a). However, the accurate understanding of the growth pattern of calcifying mollusks and the accurate interpretation of geochemical studies require a robust

identification of growth rate variations and possible periods of non biomineralization of the shell.

Among the species used in sclerochronological studies, oysters have been given particular attention. Seasonal growth rate changes can be observed based on morphological growth anomalies in the ligament area (Kirby et al. 1998), winter growth line revelation using acetate peels (Richardson et al. 1993) or natural cathodoluminescence fluctuations in modern (Langlet et al. 2006; Lartaud et al. 2010b; Doldan et al. 2018) and fossil shells (Kirby et al. 1998; Lartaud et al. 2006). Numerous studies using oxygen stable isotopes (Surge et al. 2001; Lartaud et al. 2010c; Ullmann et al. 2010; Tynan et al. 2014) or magnesium-calcium ratios (Surge and Lohmann 2008; Mouchi et al. 2013; Tynan et al. 2017) highlight the ability of oyster shells to record properly the environmental conditions, even in the fossil realm (Harzhauser et al. 2011; Bougeois et al. 2014; Huyghe et al. 2015). However, this environmental archive was shown to be altered in the shell by local environmental settings (Lartaud et al. 2010c) or by an age effect (Mouchi et al. 2013). Thus, the representativeness of mean temperatures estimated from the analyses of a single oyster hinge could be questioned. This suggests that a high-resolution investigation of growth patterns is required to better define the timing and temperature restrictions in mineralization of oyster shells. Moreover, such high-resolution studies are of paramount importance, as recent geochemical analysis methods tend to favor high spatial resolution measurements in shell materials (Meibom et al. 2007; Mouchi et al. 2013, 2018; Füllenbach et al. 2017).

Due to their economic value, the growth of the modern oyster *Magallana gigas* (former *Crassostrea gigas*) (Salvi and Mariottini 2017), has been investigated for decades. It has been found that the seasonal growth fluctuations of this species are primarily controlled by temperature, salinity and food availability (e.g. Hall 1984; Brown 1988; Gangnery et al. 2003). However, few studies have focused on the characterization and significance of the

94 growth patterns over short periods. Based on the investigation of shell sections, Langlet et al.
95 (2006) suggested that *M. gigas* form growth increments at a daily periodicity, but this study
96 was carried out in a Mediterranean lagoon were tides are reduced and oysters are continuously
97 immerged. Other studies observed increments formed at semidiurnal periods, likely produced
98 by the tidal regime in intertidal areas of the Bay of Biscay, in Atlantic waters (Higuera-Ruiz
99 and Elorza 2009). Both of these studies also revealed the existence of lower frequency growth
100 changes: every seven days in shells from the Mediterranean (Langlet et al. 2006) and within
101 fortnight cycles in shells from the Bay of Biscay (Higuera-Ruiz and Elorza 2009). In both
102 cases, only a small portion of the shell, thus a small period of time, was analyzed. To the date,
103 there is a lack of a continuous record of shell growth patterns in *M. gigas* to clearly define the
104 growth dynamics at high-resolution.
105 To understand how the sclerocronological archive can be altered by environmental
106 conditions or by the biologic activity of the organisms, we investigated the shell growth
107 pattern of *M. gigas* at high-resolution over a long-term period (i.e., 22 months). To this aim,
108 we developed a sclerochronological analysis based on cathodoluminescence increment
109 counting. Oysters studied here come from the Baie des Veys (BDV), located in Normandy
110 (France).
111
112 **Materials and methods**
113
114 The oyster *Magallana gigas*
115
116 Oysters of the species *Magallana gigas* live in shallow water and can tolerate large
117 variations of water salinity, temperature and turbidity. They are suspension feeders and filter
118 principally phytoplanktonic (diatoms) and zooplanktonic species. These oysters are

sequentially hermaphrodites and reach sexual maturity after 12 to 18 months of life in the studied area (Soletchnik et al. 1996). Reproduction occurs in the summer on the French Atlantic coast, but temperature generally remains too cold for reproduction in the BDV (Ropert et al. 2007). Thus, in the present study we will consider specimens of less than 12 months as juveniles (i.e. before summer 2005) and specimens older than 12 months as adults.

Field site and samples

In this work, we analyzed oyster shells bred on a farming site of the IFREMER (Institut Français de Recherche pour l'Exploitation de la Mer) located on the Normandy coast of the English Channel, at the Baie des Veys (BDV, 49°23.110'N 1°6.050'W; Fig. 1). The site is located in an open bay in a high intertidal setting with a semi-diurnal tidal regime (Fig. 1). Oyster spat of the species *Magallana gigas* came from wild broodstock from the Arcachon basin, located on the French Atlantic facade (Fig. 1A). They were recruited from the summer 2004 oyster farm ponds and were collected on 01/28/2005, and transplanted to the BDV on 01/29/2005 (see Lartaud et al. 2010b for further details). Then, they were allowed to breed in oyster pockets arranged on submerged tables until November 2006 (Fig. 1). The tables were located 50 cm above the sediment. Young oysters (< 1 year) were bred in 0.5 x 0.5 m pockets. Adult oysters were moved to larger pockets (1 x 0.5 m). Thus, the density of oysters remained low in the pockets throughout the experiment allowing the oysters to grow freely.

During the rearing experiment time at BDV, seawater temperature, salinity and water levels at the site were measured (data acquisition every 15 min) using a YSI multi-parameter probe attached to the oyster tables. Seawater samples for total chlorophyll *a* and pheopigment concentrations ($\mu g.l^{-1}$) were sampled fortnightly, filtered through Whatman GF/F filters to

144 estimate the trophic resources available for the oysters. Samplings were performed at low tide
145 when tide coefficients were high, which guarantieed replicable conditions.
146
147
148 ***Fig. 1***
149
150 Mn^{2+} labeling and cathodoluminescence analysis
151
152 The growth rate of *M. gigas* shells can be determined through cathodoluminescence
153 (CL) observations of the hinge area, which gathers both the complete ontogenetic record of
154 oysters and the environmental conditions experienced throughout their life (Barbin et al.
155 2008; Barbin 2013; Lartaud, et al. 2010b). The CL phenomenon results from the interactions
156 between a light-emitting centre (chemical element or impurity) and the atomic environment
157 inside the crystal lattice during excitation by an electron gun (Machel et al. 1991; Barbin and
158 Schvoerer 1997). In calcite, CL emission (~620 nm) is principally induced by the presence of
159 Mn^{2+} trapped into the lattice during mineral growth (El Ali et al. 1993; de Rafelis et al. 2000).
160 Mn^{2+} concentrations have been monitored in the BDV and showed reduced seasonal
161 fluctuations (Lartaud et al. 2010b). This work showed that in the BDV, natural CL fluctuation
162 in the shells is not linked to seawater Mn concentration but rather to seawater temperature and
163 shell growth rate.
164 For oysters, analysis of the hinge area is recommended instead of the whole shell
165 section, as it gathers the growth history on a same shell portion. Moreover, the hinge is
166 usually less impacted by shell boring species and algal deposits (Langlet et al. 2006; Lartaud
167 et al. 2010b). Additionally, the hinge portion located under the ligamental area is composed of
168 a single and more resistant microstructure (i.e., foliated calcite, Carter 1980). This is why

169 oyster hinges are more often the only shell region preserved in fossil remains and are more
170 resistant to diagenetic alterations (Lartaud et al. 2006).

171 We stained the shells 15 times at regularly spaced intervals over the 22 months
172 experiment at BDV using Mn^{2+} to obtain 15 temporal points of reference to measure shell
173 growth increments, according to the approach described in Langlet et al. (2006) (Fig. 2).
174 During low tide, the entire oyster pockets were immersed for 4 h in a tank filled with seawater
175 sampled on site with the addition of 90 $mg.l^{-1}$ of manganese chloride tetrahydrate ($MnCl_2.$
176 $4H_2O$). Once marked, the pockets were immediately returned to the culture tables. Note that
177 this protocol is not dangerous for oysters and does not affect their growth (Lartaud et al.
178 2010b).

179 Immediately after the final collection in November 2006, the specimens were
180 sacrificed, and the shells were sectioned and mounted on slides for CL microscopy, as
181 described in Lartaud et al. (2010b).

182 The slides were observed with a cold cathode (Cathodyne-OPEA, 15-20 kV and 200
183 to 400 $\mu A.mm^{-2}$ under a pressure of 0.05 Torr) to reveal both the natural luminescence
184 variability in the shells and the Mn labels (Fig. 3). A Nikon D5000 (1400 ASA) camera was
185 used for luminescence image acquisition with a constant exposure time of 20 s. The analysis
186 of growth intervals was conducted using the CL-mounted photographs with Adobe Photoshop
187 CS6 image processing software. Mounted photographs, providing a complete and detailed
188 panorama of the hinge area, were used to generate luminescence spectra by means of ImageJ
189 software (Fig. 3B). Luminescence analyses are semi-quantitative because each shell has its
190 own heterogeneity, which makes luminescence intensity normalization impossible (Langlet,
191 et al. 2006; Lietard and Pierre 2008). Luminescence intensity is therefore expressed in
192 arbitrary units (AU).

For each shell, the Mn^{2+} marking recognition allowed us to transform CL spectra along a growth profile into a calendar profile (Lartaud et al. 2010b; Mouchi et al. 2013). The least-squares method for non-linear regression analysis, following the Levenberg-Maquardt method (Statistica software), was performed to estimate parameters of the Von Bertalanffy relationship of oyster hinges growth. This equation enables the estimation of ontogenetic ages from shell hinge lengths:

$$L_t = L\infty\ (1 - e^{-k(t - t0)}) \qquad \text{(equation 1)}$$

where Lt is the hinge shell length (mm) at time t (in years), L∞ is the maximum hinge shell length (mm), t_0 (in years) is the setting size and k is a time constant. It is then possible to determine the maximum size of the shell, as a linear relationship between hinge length and shell length size that was previously shown for oysters at the BDV (Lartaud et al. 2010b).

Analysis of the shell growth rate at higher resolution (i.e., at the scale of the calcite increment) corresponded to the study of micrometric alternations between highly luminescent and dull calcite CL increments (Fig. 3C). We defined a pair of bright-dull bands observed under CL as a CL increment. We counted the number of these pairs of bright-dull increments and measured the width between two successive bright increments with ImageJ to build sclerochronological profiles and determine high-resolution growth patterns of the shells throughout their lives (Nedoncelle et al. 2013).

Fig. 2 & 3

Principal component analysis

To examine which parameters controls the growth of oysters at high resolution, a Principal Component Analysis (PCA) was carried out using the software Matlab. The PCA was performed based on increment width fluctuation with respect to mean daily temperature, salinity, immersion duration, high tide level and low tide level.

Fast Fourier Transform analysis

The variability in growth increment width was analyzed via a spectral analysis, based on Fast Fourier Transform (FFT). In Matlab, we used the multi-taper method (Thomson 1982) and robust red noise modeling, as implemented in the singular spectrum analysis multi-taper method (SSA-MTM) toolkit (Ghil et al. 2002).

Mann-Whitney test

The Mann-Whitney test was used for comparison between mean growth rate between winter and summer and to determine if these values are statistically different or not. Before using this non-parametric test, the non-respect of the normality and homoscedasticity conditions were checked using the Shapiro and Bartlett tests respectively.

Results

Fluctuation Baie des Veys environmental parameters

242 We report the fluctuation of temperature, salinity, chorophyll *a*, pheopigments
243 concentration and tides measured in the BDV on Fig. 2. The temperature exhibited seasonal
244 cyclic variations with minimum and maximum values of 5 °C between January and March
245 and 20 °C from July to September, respectively. Salinity remained almost constant throughout
246 the year at a value of ~ 33-34 psu with isolated transient decreases (~29 – 31 psu) due to
247 freshwater input in response to elevated rainfall events.
248 Concentrations of chlorophyll *a* and pheopigments, assumed proxies of food available
249 for oysters, are also reported in Fig. 2. Pheopigment concentrations remained low (< 2 mg/m^3)
250 during the whole interval compared to chlorophyll *a* concentrations, which fluctuated between
251 0.5 mg/m^3 and 11.5 mg/m^3. The higher concentrations were reached during phytoplanktonic
252 blooms, which occurred mainly during spring. We also calculated the ratio between
253 chlorophyll *a* and pheopigment concentration, which is related to the quality of food for
254 oysters (Le Guitton et al. 2015; Belley et al. 2016). This ratio is mostly driven by the
255 concentration in chlorophyll *a* and is thus high during spring and the end of summer and low
256 during winter.
257 Variations in the high tide level ranged between 3 and 6 m (mean = 4 m) above the
258 oyster tables, whereas the low tides ranged between -0.5 and 2 m (mean = 0.5 m) (Fig. 3).
259 Thus, oysters remained completely immersed when tidal coefficients were low and could be
260 exposed during 3 h when tidal coefficients were high.
261
262
263 General trends of hinge growth rates
264
265 The cumulative change of the hinge lengths measured between the successive
266 markings on 11 shells is reported on Fig. 4. It highlights that the total hinge lengths ranged

267 between 13 and 21 mm after 22 months of growth. The growth of all oyster shells followed a
268 Von Bertalanffy model (r = +0.99, p = 0.01 n = 157), with a fast growth rate during the
269 beginning of their lives and a progressive slowing of growth as they mature, as observed for
270 other oysters (Bayne and Newell 1983; Mitchell et al. 2000). The Von Bertalanffy growth
271 function revealed an expected maximum hinge length of 27.6 mm for *M. gigas* shells at BDV.
272 These measurements yield similar results to many other works on oysters including previous
273 investigations in the BDV (Lartaud et al. 2010b) suggesting that the growth of the studied
274 oysters was not disrupted by any unusual environmental or endogenous factors.
275
276 ***Fig. 4***
277
278 Figure 5 presents the variation of the mean growth rate of the 11 oyster hinges
279 between the successive Mn^{2+} markings and the mean daily seawater temperature. The general
280 pattern of growth exhibited seasonal variations. The first part of the profile (i.e., February
281 2005) showed high variability in growth rates, leading to low values (mean of 25 ± 15
282 μm/day) immediately after transplantation. Very high values were observed during the rest of
283 the month (120 ± 60 μm/day). During the rest of 2005, mean growth rate fell to ~ 20 ± 7
284 μm/day from March to July and then increased during summer, with a maximum of ~ 50 ± 13
285 μm/day observed in September – October. Then, shell growth decreased during the winter to
286 minimum values of 8 ± 2 μm/day in February 2006, followed by a slightly but significant
287 increase through the summer of 2006, reaching 24 ± 8 μm/day. Mann-Whitney U test (n = 81,
288 p< 0.001) revealed that this increase between winter and summer values is statistically
289 significant. The mean growth rate immediately before collection in November 2006 was 12 ±
290 5 μm/day.
291

292 ***Fig. 5***

293

294 Figure 6 presents correlations between the mean growth rates and the mean
295 temperature as well as the chlorophyll *a* concentration, calculated between the markings.
296 Growth rate changes were consistent with the seasonal pattern of seawater temperatures,
297 except for the youngest part (i.e., during the second half of February 2005), which showed
298 high variability and high values in shell growth rates although temperatures remained low.
299 Growth outlier of February 2005 was removed from comparison with environmental
300 parameters. A low but positive correlation was observed between the mean shell growth rates
301 and temperatures (Least mean squares regression, $r = +0.52$, $p = 0.05$; Fig. 6) and highlights
302 that the extreme growth value of February 2005 is thus non-influenced by temperature
303 variations (Fig. 6).

304 Unfortunately, chlorophyll *a* was not monitored during the high growth rate value of
305 February 2005, but in the rest of the whole experiment, there was no relationship with shell
306 growth rate (Least mean squares regression, $r = +0.001$, $p = 0.89$; Fig. 6), suggesting that this
307 parameter has a lower influence on the shell growth rate compared to temperature.

308

309 ***Fig. 6***

310

311 High-resolution growth patterns

312

313 Several specimens revealed a quasi-continuous record of CL increments during the
314 two year monitoring and we counted the number of increments and measured the fluctuation
315 of the increment widths for nine shells when CL observations were of quality (Table 1). The
316 inferred sclerochronological profiles are presented in Fig. 7 for samples BDV3 and BDV5,

317 which present the most complete record (Table 1). Positions of Mn^{2+} chronological markings
318 were reported on Fig. 7. The overall pattern of increment widths observed on Fig. 7 has five
319 distinct periods. During the first period, in February 2005, the mean increment width was
320 intermediate (31 ± 14 μm for BDV3 and 17 ± 5 μm for BDV5) and increased during a second
321 period from March to September (45 ± 24 μm for BDV3 and 50 ± 19 μm for BDV5). Then, a
322 third period showed a decrease in increment width from September 2005 to November 2005,
323 reaching 32 ± 20 μm for BDV3 and 32 ± 10 μm for BDV5. Although the identification and
324 measurement of increment widths were not possible for BDV3 from November 2005 to
325 March 2006, due to very dull luminescence of the hinge, specimen BDV5 allowed increment
326 counting to the end of January 2006. This fourth period corresponds to the beginning of
327 winter and was marked by low mean increment width values (10 ± 6 μm). No measurements
328 were possible from February to May 2006 for specimen BDV5, because the width between
329 two successive increments was too small to be clearly distinguishable from each other. For
330 BDV3, values remained low from March to May 2006 (mean of 9 ± 3 μm/inc.), but displayed
331 higher fluctuations (from 5 to 20 μm/inc.) compared to the beginning of winter. During the
332 fifth period (May to November 2006), the mean value of increment widths was high (mean of
333 20 ± 9 μm for BDV3 and 18 ± 8 μm for BDV5) and highly variable (between 3 and 58 μm).
334 The number of CL increments secreted per day (inc./day) between two successive
335 chemical markings was estimated from the analysis of nine shells (Table 1) and is reported for
336 samples BDV3 and BDV5 on Fig. 7. The mean number of increments per day was variable
337 according to the period considered. First, during February, a mean of 5.2 ± 2.2 inc./day was
338 calculated. The formation of infra-daily increments was highlighted by the duplication of the
339 staining on 02/09/2005 (Fig. 8), corresponding to increment mineralization in less than four
340 hours, the duration of the Mn^{2+} bath. From the end of February to September 2005, a mean of
341 0.8 ± 0.1 inc./day was secreted. From September to November 2005, the number of

342 increments per day increased to 1.7 ± 0.1. During the following winter and the beginning of
343 spring, when increment counting was possible from November 2005 to January 2006 and
344 from March to May 2006, the daily biomineralization rhythm fell to 1.6 ± 0.1 inc./day. Finally,
345 from May to November 2006, 1.8 ± 0.2 inc./day were secreted. Except for February 2005,
346 where numerous infra-daily increments occurred, the number of increment formed per day
347 during the adult period (~ 2 increments per day) was significantly higher than in the oysters of
348 < 1 year old (> 1 increment per day) (Student test, n = 34, p< 0.001).
349
350 ***Fig. 7, Fig. 8, Table 1***
351
352 **Discussion**
353
354 Drivers of oyster shell growth
355
356 The analysis of growth increments formed during a 22 month *in situ* experiment
357 revealed three distinct patterns. During February 2005, the oysters mineralized more than 5
358 increments per day. From the end of February to September 2005, corresponding to oysters
359 aged 6 to 12 months, less than one increment per day was mineralized, with variability in the
360 increment width. During the third period (September 2005 to November 2006),
361 corresponding to oysters more than one year old, shells formed almost two increments per day,
362 likely tide-related, as BDV has a semi-diurnal tide regime.
363 Circatidal growth patterns are frequently observed in bivalves from intertidal areas,
364 such as the cockle *Cerastoderma edule* (Mahé et al. 2010), the mussel *Mytilus edulis*
365 (Richardson 1989) and the clam *Chione cortezi* (Schöne et al. 2002a). Circatidal structures
366 result from shell accretion during high tides, associated with periods of active pumping in

367 well-oxygenated waters, and growth cessation at low tides, during aerial exposure, when
368 animals close their shells tightly leading to anaerobic conditions and internal pH
369 modifications (Lutz and Rhoads 1977). Based on microscopic observations of small portions
370 of shell sections deposited during spring, the increments of ~10 μm found by Higuera-Ruiz
371 and Elorza (2009) in the hinge area of *M. gigas* shells from intertidal zones of the Bay of
372 Biscay were attributed to tidal periodicity. Our results thus support the growth model defined
373 by these authors, adding an observation of growth increment over a long period (i.e., > 1 year).
374 It is interesting to note that both bright and dull CL increments are formed during one tidal
375 cycle. But at this stage it is unclear if a bright band corresponds to the flood or ebb current or,
376 as oysters are not necessarily emerged at each tide in the studied area, to the maximum or
377 minimum tide levels. Moreover, the process that drives the mineralization of bright and dull
378 increments seems to be more difficult to explain during the youngest part of the life of the
379 oysters, as they are able to mineralize two bright growth lines, i.e., two CL growth lines in a
380 tank where tides are not recorded. It implies that processes other than environmental ones,
381 probably related to biological factors, influence the mineralization of the CL increments. It
382 also confirms that, at this scale, bright and dull intervals are not related to natural fluctuation
383 of the Mn^{2+} concentration in seawater.

384 Our results contrast with the observations made by Langlet et al. (2006), which
385 showed a single CL increment formed per day in *M. gigas* shells from Thau lagoon on the
386 Mediterranean coast. In this area where tide fluctuations are only a few centimeters, oysters
387 remain continuously submerged. Thus, a complex combination of other parameters,
388 particularly evaporation and wind regimes, including the diurnal cycle of wind velocity
389 (Bouin et al. 2012), together with the functioning of artificial channels connecting to
390 Mediterranean seawaters, substantially modify the hydrology of the lagoon and can generate
391 daily rather than tidal changes in the water masses (Audouin 1962).

392 Based on the observations described above, we can assume that oysters form two
393 increments per day during the second year of life in our study. Thus, the decrease observed of
394 this ratio to 1.5 to 1.6 inc/day during the winter to early spring period, a time when shell
395 growth rate was reduced, suggests (1) that all CL growth increments may not be countable
396 due to extremely reduced width and brightness and/or (2) not all increments are formed
397 related to occasional growth breaks. CL increments were clearly distinguishable during the
398 March to May 2006 period. Thus, the fact that oysters mineralize less than 2 inc./day cannot
399 be explained by inaccurate observation of the shell, Thus, one can argue in favor of the
400 second hypothesis. Occasional growth cessations are consistent with the model described by
401 Schöne (2008) for shells from high-intertidal areas, leading to an incomplete record for
402 several days. Observations done on the shell of the bivalve *C. cortezi* demonstrated that
403 growth is slower during spring cool nights (Schöne et al. 2002a). The growth cessations
404 observed during winter and spring for *M. gigas* could reflect these kinds of stressful
405 conditions corresponding to occasional but significantly lower temperatures.
406 We analyzed the variability in growth increment width via FFT spectral analysis.
407 Based on tide-related growth increments (i.e. 2 inc./day), this analysis revealed two
408 periodicities of 64 and 28 to 32 increments corresponding to growth rhythms of 32 and 14 to
409 16 days. The ~15 days frequency relates to the fortnight cycle, while the 32 days frequency
410 can be attributed to the synodic lunar cycle (29.5 days). Similar growth patterns have been
411 observed in the Mg/Ca ratio of *M. gigas* oyster shells (Higuera-Ruiz and Elorza 2009; Mouchi
412 et al. 2013) and are likely highlighted by the formation of dark/clear bands in the umbo
413 (Higuera-Ruiz and Elorza 2009). However, to date, the description of such growth patterns in
414 the shell mineralization has not been performed for such an extended period of time. Lunar
415 cycles in the shell mineralization can be related to valve activity, with an increase in the
416 duration of valve opening during highest tides and a decrease during the lowest ones (Tran et

417 al. 2011), and/or the role of current velocity changes, which modify food availability (Clark
418 2005; Lartaud et al. 2010a).

419 For BDV3 and BDV5, a comparison of the variability of CL increment width when ~2
420 increments were mineralized per day and the high tide sea level reveals that both for the
421 autumn 2005 and spring to autumn 2006 periods, the larger increment width correlates most
422 of the time with periods of lower high tide levels (Fig. 9; reversed scale), that occur a few
423 days after neap tides in the BDV. In contrast, a narrow increment width coincides with higher
424 high tide levels, which occur just after spring tides. However, we note two exceptions: the full
425 moon of the 09/18/05 and the new moon of the 09/22/06, when large increment widths are
426 observed. Contrary to the descriptions made by Schöne (2008) in high-intertidal areas, oyster
427 shell production is favored at neap tides compared with spring tides. This is consistent with
428 the pattern proposed by Ohno (1989) for oyster shells from mid- to low-intertidal settings, as
429 also illustrated by observations on *C. cortezi* (Schöne et al. 2002a) and *Adamussium colbecki*
430 (Lartaud et al. 2010a).

431 To test these assumptions and to better determine the causes of the increment widths
432 fluctuation, we analyzed the relationship between this parameter and the mean daily
433 temperature, salinity, immersion duration, high tide level and low tide level for samples
434 BDV3 and BDV5 for periods when ~2 increments were mineralized per day using a Principal
435 Component Analysis (PCA; Fig. 10). This analysis indicated that increment width is not
436 correlated with salinity variations, immersion duration, high tide level or low tide level for
437 both oysters. However, it highlights a correlation with temperature, which was greater during
438 2005 than 2006.

439 Thus, seawater temperature variation seems to be the most important factor controlling
440 increment width. There is also evidence that the seasonal changes in growth rates are
441 primarily driven by temperature (Fig. 5), and various studies report the role of temperature in

increment width variation, such as for the giant clam *Hippopus hippopus* (Schwartzmann et al. 2011) or the king scallop *Pecten maximus* (Chauvaud et al. 1998). At the CL increment width resolution, this relationship is obvious for 2005 but less for 2006, where increment width fluctuation seems to be correlated with high tide level (Fig. 9). Thus temperature changes in the BDV seawaters alone cannot explain small-scale growth variability in oyster shells. Cloern (1991) showed that during spring tides, phytoplankton concentration is dissipated by current flow velocity, which could lead to less available food and/or more energy consumption for shell growth during this period. Phytoplankton concentration can therefore appear as a secondary growth driver, when temperature is not a limiting factor.

Fig. 9, Fig. 10

Winter and early spring growth

The winter and spring periods of the second year are characterized by a slight decrease in the number of increments mineralized each day compared to the summer period (Fig. 7). We observe that the decrease in shell growth during the winter results from both a decrease in the number of increments and the deposition of narrower increments (Fig. 5 and 7). This decrease in growth rate, likely related to the relationship between oyster shell growth and temperature and, possibly, in a second order to food availability, has already been documented for oyster species and in particular for *M. gigas* (Brown and Hartwick 1988; Mitchell et al. 2000). The minimum temperature at which oysters stop mineralizing their shells is, however, subject to debate. Quayle (1988) and Kirby et al. (1998) set this temperature boundary near 10°C from the study of modern Eastern and Pacific oyster specimens. According to Ullmann et al. (2010), oysters should stop biomineralization when

467 seawater temperature is below 6°C. Here, we observed that oysters mineralize their shells
468 even during winter (Fig. 4). In the BDV, the coldest interval occured between the markings of
469 the end of January and March, with a mean temperature of 5.9°C (Fig. 5). Between these two
470 markings, temperatures ranged between 6.8 and 5°C. Thus, it is likely that oysters are able to
471 mineralize their shells at least to a temperature of 6.8°C and even possibly to ~ 5°C. This
472 observation is of crucial importance for paleoenvironmental reconstructions, because it shows
473 that oysters are potentially good indicators for estimating cold seawater temperatures, as low
474 as ~ 6°C.
475
476 Juvenile growth patterns
477
478 In our study, during most of the first year of their life i.e. before reaching their sexual
479 maturity (January to September 2005), oysters exhibited completely different shell growth
480 patterns compared with the rest of the studied life history. Increment counting pointed out the
481 formation of several increments each day (mean of ~5±2 inc./day) in February 2005. Then
482 from March to September 2005, less than one increment mineralized per day instead of two in
483 the adult period (see above). Although we have only one cohort - which limits extrapolations
484 to a general feature at the species level - this different pattern during the juvenile stage was
485 observed for all shells analyzed. CL increments were easily identifiable and bias in increment
486 counting cannot explain this observation. Measurements of the environmental parameters
487 (temperature, salinity and food availability) do not indicate different specific conditions
488 compared to the second year of the experiment (Fig. 2) and no elevated mortality (> 10 %)
489 was reported in the BDV breeding station during the experiment (Mary et al. 2006; Ropert et
490 al. 2007).

491 Nearly one growth increment mineralized per day has also been reported in the shell
492 of the bivalve *C. cortezi* (Goodwin et al., 2001; Schöne et al., 2002b), but to date the drivers
493 remain unknown. Interestingly, the formation of numerous growth increments per day during
494 the February 2005 period coincides with high shell growth rates (Fig. 4). This pattern could
495 be the consequence of unusual environmental conditions in the BDV during February 2005,
496 but the parameters monitored do not exhibit any such anomalies. Additionally, a similar high
497 shell growth rate has been identified in other oysters bred in different sites on the French
498 Atlantic coast and coming from the same spat as the ones analyzed in this work (Lartaud et al.,
499 2010b). However, in the other sites, the growth peak occured when the oysters were three to
500 four months older (i.e. during the spring). Moreover, the hinge length mineralized between
501 02/09/05 and 02/24/05, which varies significantly according to the individuals, is a function
502 of the number of increments produced (Fig. 11). It is thus difficult to directly relate the shell
503 growth of oysters to environmental parameters during this period, and should rather imply
504 internal biological processes such as physiological factors and/or genetic features, as
505 suggested by Rodland et al. (2006) based on the analysis of behavior patterns of bivalves at
506 ultradian time-scales.
507 From the end of February to September 2005, the absence of a bi-daily rhythm in
508 increment formation corresponds to periodic growth cessations. However, during the first
509 year of life, increment widths are larger compared to the second year of life (Fig. 7), which is
510 consistent with a Von Bertalanffy growth model (Berthome et al. 1986; Brown and Hartwick
511 1988; Mitchell et al. 2000). This suggests that shells grew more rapidly, but less frequently
512 during the first months of life, corresponding to a fast growth but not at each tide (i.e., less
513 than half of the tidal increments are recorded).
514 It is still unclear why young oysters exhibit such growth patterns, with a growth
515 history more discontinuous than during the adult phase. The impact of energy budget

allocation to sexual reproduction and gamete production instead of shell mineralization cannot be invoked as a possible cause, as oysters had not yet reached sexual maturity in the spring of 2005. This metabolic trait occurs after 12 to 18 months of life (Soletchnik et al. 1996). However, this emphasizes the importance of input provided by a sclerochronological approach, compared to measurements resulting from mark and recapture techniques only, because the former provides a better description of growth evolution at fine scale. Thus, oysters have a more complete record of their environmental conditions after the first year of life and more precisely during summer and autumn periods, with less growth breaks and shell biomineralization during each tide.

Fig. 11

Conclusions

Based on a cathodoluminescence approach, this study provides the longest high-resolution record of growth in oyster shells, showing two distinct patterns. The general feature is the formation of circatidal CL growth increments, composed of a pair of bright/dull luminescent bands likely tide-related, and associated with semi-lunar and lunar growth rate changes. A seasonal trend shows growth rate decrease, with growth cessations in winter, even if oysters are able to mineralize at temperatures of ~5°C. In addition, our *in situ* experiment suggests variable growth patterns during the first months of life, characterized by either (1) numerous infra-daily growth increments or (2) frequent growth breaks during the younger period (below 1 year old), despite high annual shell growth rates. These unconventional growth patterns require further investigations.

Considering the contribution of CL analysis in growth increment revelation, these results are of particular interest for ecological studies of bivalves in general and oysters in particular, but also for the use of the shells as (paleo)environmental proxies. Indeed, shell growth rate changes and growth cessations at high-resolution, should be taken into account for paleoclimatic reconstructions based on growth indices or geochemical proxies. The numerous growth cessations observed during the first months of life can lead to misinterpretations in the reconstruction of environmental conditions. Therefore, we recommend to avoid sampling this period in further paleoenvironmental and paleoclimatic studies.

Acknowledgments

This work was financially supported by the ANR Amor 'Data Model Reconstruction of the Cenozoic Climate' and the BQR project from Sorbonne Université, 'High frequency to very high frequency recordings of environmental changes to climate by biomineralization.' Special thanks may be due to Brian Mitchell for improving the English of the manuscript. Thoughtful comments by Editor A. Checa and two anonymous reviewers helped to improve the original version of the manuscript.

Compliance with ethical standards

Conflict of interest The authors declare that they have no conflict of interest.

Ethical approval All applicable international, national, and/or institutional guidelines for the care and use of animals were followed.

565 **References**

566

567 Audouin J (1962) Hydrologie de l'étang de Thau. Rev Trav Inst Pech Marit 26(2): 5-104

568 Barbin V (2013) Application of cathodoluminescence microscopy to recent and past
569 biological materials: a decade of progress. Mineral Petrol 107(3): 353-362

570 Barbin V, Schvoerer M (1997) Cathodoluminescence and geosciences. C R Acad Sci Paris
571 325: 157–169

572 Barbin V, Ramseyer K, Elfman M (2008) Biological record of added manganese in seawater:
573 a new efficient tool to mark in vivo growth lines in the oyster species *Crassostrea*
574 *gigas*. Int J Earth Sci 97(1): 193-199

575 Bayne BL, Newell RIE (1983) Physiological energetics of marine molluscs. In The Mollusca:
576 Physiology, Part 1. (ed. A.S.M. Saleuddin and K.M. Wilbur), Academic Press, pp 407-
577 415

578 Belley R, Snelgrove PV, Archambault P, Juniper SK (2016) Environmental drivers of benthic
579 flux variation and ecosystem functioning in Salish Sea and Northeast Pacific
580 sediments. PloS 11(3): e0151110

581 Berthome JP, Prou J, Bodoy A (1986) Performances de croissance de l'huître creuse,
582 *Crassostrea gigas* (Thunberg) dans le bassin d'élevage de Marennes-Oléron entre 1979
583 & 1982. Haliotis 15: 183-192

584 Bougeois L, de Rafelis M, Reichart GJ, de Nooijer LJ, Nicollin F, Dupont-Nivet G (2014) A
585 high resolution study of trace elements and stable isotopes in oyster shells to estimate
586 Central Asian Middle Eocene seasonality. Chem Geol 363: 200–212

587 Bouin MN, Caniaux G, Traulle O, Legain D, Le Moigne P (2012) Long-term heat exchanges
588 over a Mediterranean lagoon. J Geophys R: Atmospheres 117(D23)

589 Brown JR (1988) Multivariate analyses of the role of environmental factors in seasonal and
590 site-related growth variation in the Pacific oyster *Crassostrea gigas*. Mar Ecol Prog Ser
591 45(3): 225-236

592 Brown JR, Hartwick EB (1988) Influences of temperature, salinity and available food upon
593 suspended culture of the Pacific oyster, *Crassostrea gigas*: I. Absolute and allometric
594 growth. Aquaculture 70(3): 231-251

595 Butler PG, Wanamaker Jr, AD, Scourse JD, Richardson CA, Reynolds DJ (2013) Variability
596 of marine climate on the North Icelandic Shelf in a 1357-year proxy archive based on
597 growth increments in bivalve *Arctica islandica*. Palaeogeogr Palaeoclimatol Palaeoecol
598 373: 141–151

599 Carter, JG, 1980. Guide to bivalve shell microstructures. In: Rhoads, D.C. and Lutz, R.A.
600 (Eds), Skeletal growth of aquatic organisms. Plenum Press, New York: 645-673

601 Chauvaud L, Thouzeau G, Paulet YM (1998) Effects of environmental factors on the daily
602 growth rate of *Pecten maximus* juveniles in the Bay of Brest (France). J Exp Mar Biol
603 Ecol 227(1): 83-111

604 Chauvaud L, Lorrain A, Dunbar RB, Paulet YM, Thouzeau G, Jean F, Guarini JM,
605 Mucciarone D (2005) Shell of the Great Scallop *Pecten maximus* as a high frequency
606 archive of paleoenvironmental change. Geochem Geophys Geosyst 6: 1–34

607 Clark GR (2005) Daily growth lines in some living Pectens (Mollusca: Bivalvia), and some
608 applications in a fossil relative: time and tide will tell. Palaeogeogr Palaeoclimatol
609 Palaeoecol 228(1): 26-42

610 Cloern JE (1991) Tidal stirring and phytoplankton bloom dynamics in an estuary. J Mar
611 Res 49(1): 203-221

612 de Rafelis M, Renard M, Emmanuel L, Durlet C (2000) Apport de la cathodoluminescence à
613 la connaissance de la spéciation du manganèse dans les carbonates pélagiques. C R
614 Acad Sci Paris 330: 391–398
615 Dettman DL, Flessa KW, Roopnarine PD, Schöne BR, Goodwin DH (2004) The use of
616 oxygen isotope variation in shells of estuarine mollusks as a quantitative record of
617 seasonal and annual Colorado River discharge. Geochim Cosmochim Acta 68:1253–
618 1263
619 Doldan MS, de Rafelis M, Kroeck MA, Pascual MS, Morsan EM (2018) Age estimation of
620 the oyster *Ostrea puelchana* determined from the hinge internal growth pattern. Mar Biol
621 165: 119
622 El Ali A, Barbin V, Calas G, Cervelle B, Ramseyer K, Bouroulec J (1993) Mn^{2+} activated
623 luminescence in dolomite, calcite and magnesite: quantitative determination of
624 manganese site distribution by EPR and CL spectroscopy. Chem Geol 104 : 189–202
625 Evans JW (1972) Tidal growth increments in the cockle *Clinocardium nuttalli*. Science 176:
626 416–417
627 Füllenbach CS, Schöne BR, Shirai K, Takahata N, Ishida A, Sano Y (2017) Minute co-
628 variations of Sr/Ca ratios and microstructures in the aragonitic shell of *Cerastoderma*
629 *edule* (Bivalvia) - Are geochemical variations at the ultra-scale masking potential
630 environmental signals? Geochim Cosmochim Acta 205: 256-271
631 Gangnery A, Chabirand J-M, Lagarde F, Le Gall P, Oheix J, Bacher C, Buestel D (2003)
632 Growth model of the Pacific oyster, *Crassostrea gigas*, cultured in Thau Lagoon
633 (Méditerranée, France). Aquaculture 2015: 267-290
634 Ghil M, Allen RM, Dettinger MD, Ide K, Kondrashov D, Mann ME, Robertson A, Saunders
635 A, Tian Y, Varadi F, Yiou P (2002) Advanced spectral methods for climatic time series.
636 Rev Geophys 40: 31-341

637 Goodwin DH, Flessa KW, Schöne BR, Dettman DL (2001) Cross-calibration of daily growth
638 increments, stable isotope variation, and temperature in the gulf of California bivalve
639 mollusk *Chione cortezi*: implications for paleoenvironmental analysis. Palaios 16: 387–
640 398.
641 Goodwin DH, Schöne BR, Dettman DL (2003) Resolution and fidelity of oxygen isotopes as
642 paleotemperature proxies in bivalves mollusk shells: models and observations. Palaios
643 18: 110-125.
644 Gröcke DR, Gillikin DP (2008) Advances in mollusc sclerochronology and sclerochemistry:
645 tools for understanding climate and environment. Geo-Marine Lett 28: 265–268
646 Hall S (1984) A multiple regression model of oyster growth. Fish Res 2: 167-175
647 Harzhauser M, Piller WE, Müllegger S, Grunert P, Micheels A (2011) Changing seasonality
648 patterns in Central Europe from Miocene Climate Optimum to Miocene Climate
649 Transition deduced from the *Crassostrea* isotope archive. Global Planet Change 76: 77-
650 84, doi: 10.1016/j.gloplacha.2010.12.003
651 Higuera-Ruiz R, Elorza J (2009) Biometric, microstructural, and high-resolution trace
652 element studies in *Crassostrea gigas* of Cantabria (Bay of Biscay, Spain):
653 Anthropogenic and seasonal influences. Estuar Coast Shelf Sci 82(2): 201-213
654 Hudson JH, Shinn EA, Halley RB, Lidz B (1976) Sclerochronology: a tool for interpreting
655 past environments. Geology 4: 361–364
656 Huyghe D, Lartaud F, Emmanuel L, Merle D, Renard M (2015) Palaeogene climate evolution
657 in the Paris Basin from oxygen stable isotope ($\delta^{18}O$) compositions of marine molluscs. J
658 Geol Soc 172(5): 576-587
659 Ivany LC, Lohmann KC, Hasiuk F, Blacke DB, Glass A, Aronson RB, Moody RM (2008)
660 Eocene climate record of a high southern latitude continental shelf: Seymour Island,
661 Antarctica. Geol Soc Am Bull 120: 659-678

662 Kirby MX, Soniat TM, Spero HJ (1998) Stable isotope sclerochronology of Pleistocene and
663 Recent oyster shells (*Crassostrea virginica*). Palaios 13: 560–569

664 Krantz DE, Williams DF, Jones DS (1987) Ecological and paleoenvironmental information
665 using stable isotope profiles from living and fossil molluscs. Palaeogeogr
666 Palaeoclimatol Palaeoecol 58(3-4): 249-266

667 Langlet D, Alunno-Bruscia M, Rafélis M, Renard M, Roux M, Schein E, Buestel D (2006)
668 Experimental and natural cathodoluminescence in the shell of *Crassostrea gigas* from
669 Thau lagoon (France): ecological and environmental implications. Mar Ecol Prog
670 Ser 317: 143-156

671 Lartaud F, Langlet D, De Rafelis M, Emmanuel L, Renard M (2006) Description of seasonal
672 rythmicity in fossil oyster shells *Crassostrea aginensis* Tournouer, 1914 (Aquitanian)
673 and *Ostrea bellovacina* Lamarck, 1806 (Thanetian). Cathodoluminescence and
674 sclerochronological approaches. Geobios 39(6): 845-852

675 Lartaud F, Chauvaud L, Richard J, Toulot A, Bollinger C, Testut L, Paulet YM (2010a)
676 Experimental growth pattern calibration of Antarctic scallop shells (*Adamussium*
677 *colbecki*, Smith 1902) to provide a biogenic archive of high-resolution records of
678 environmental and climatic changes. J Exp Mar Bio Ecol 393(1): 158-167

679 Lartaud F, de Rafélis M, Ropert M, Emmanuel L, Geairon P, Renard M (2010b) Mn labelling
680 of living oysters: artificial and natural cathodoluminescence analyses as a tool for age
681 and growth rate determination of *C. gigas* (Thunberg, 1793) shells. Aquaculture 300(1):
682 206-217

683 Lartaud F, Emmanuel L, de Rafelis M, Ropert M, Labourdette N, Richardson CA, Renard M
684 (2010c) A latitudinal gradient of seasonal temperature variation recorded in oyster
685 shells from the coastal waters of France and The Netherlands. Facies 56: 13–25

686 Le Guitton M, Soetaert K, Damsté JS, Middelburg JJ (2015) Biogeochemical consequences of
687 vertical and lateral transport of particulate organic matter in the southern North Sea: a
688 multiproxy approach. Estuar Coast Shelf Sci 165: 117-127

689 Lietard C, Pierre C (2008) High-resolution isotopic records ($\delta^{18}O$ and $\delta^{13}C$) and
690 cathodoluminescence study of lucinid shells from methane seeps of the Eastern
691 Mediterranean. Geo-Mar Lett 28(4): 195-203

692 Lutz RA, Rhoads DC (1977) Anaerobiosis and a theory of growth line formation. Science
693 198(4323): 1222–1227

694 Machel HG, Mason RA, Mariano AN, Mucci A (1991) Causes and emission of luminescence
695 in calcite and dolomite, and their applications for studies of carbonates diagenesis. In:
696 Barker, C.E., Kopp, O.C. (Eds.), Luminescence Microscopy: Quantitative and
697 Qualitative Aspects. SEPM 25: 9–25

698 Mahé K, Bellamy E, Lartaud F, de Rafélis M (2010) Calcein and manganese experiments for
699 marking the shell of the common cockle (*Cerastoderma edule*): tidal rhythm validation
700 of increments formation. Aquat Living Resour 23(3): 239-245

701 Mary C, Pien S, Ropert M, Blin J-L (2006) Rapport REMONOR, Résultats 2005, Ifremer, 67
702 pp.

703 Meibom A, Mostefaoui S, Cuif JP, Dauphin Y, Houlbreque F, Dunbar R, Constantz B (2007)
704 Biological forcing controls the chemistry of reef-building coral skeleton. Geophys Res
705 Lett 34(2): 1-5

706 Mitchell IM, Crawford CM, Rushton MJ (2000) Flat oyster (*Ostrea angasi*) growth and
707 survival rates at Georges Bay, Tasmania (Australia). Aquaculture 191(4): 309-321

708 Mouchi V, de Rafélis M, Lartaud F, Fialin M, Verrecchia E (2013) Chemical labelling of
709 oyster shells used for time-calibrated high-resolution Mg/Ca ratios: a tool for estimation

of past seasonal temperature variations. Palaeogeogr Palaeoclimatol Palaeoecol 373: 66-74

Mouchi V, Briard J, Gaillot S, Argant T, Forest V, Emmanuel L (2018) Reconstructing environments of collection site from archaeological bivalve shells: case study from oysters (Lyon, France). J Archaeol Sci: Reports 21 : 1225-1235, doi: 10.1016/j.jasrep.2017.10.025

Nedoncelle K, Lartaud F, de Rafélis M, Boulila S, Le Bris N (2013) A new method for high-resolution bivalve growth rate studies in hydrothermal environments. Mar Biol 160(6): 1427-1439

Nedoncelle K, Lartaud F, Contreira Pereira L, Yücel M, Thurnherr AM, Mullineaux L, Le Bris N (2015) *Bathymodiolus* growth dynamics in relation to environmental fluctuations in vent habitats. Deep Sea Res I Oceanogr Res Pap 106: 183–193

Ohno T (1989) Palaeotidal characteristics determined by micro-growth patterns in bivalves. Palaeontology 32(2): 237-263

Quayle DB (1988) Pacific oyster culture in British Columbia. Can Bull Fish Aquat Sci 218: 241

Richardson CA (1989) An analysis of the microgrowth bands in the shell of the common mussel *Mytilus edulis*. J Mar Biol Assoc U K 69(2): 477-491

Richardson CA, Collis SA, Ekaratne K, Dare P, Key D (1993) The age determination and growth rate of the European flat oyster, *Ostrea edulis*, in British waters determined from acetate peels of umbo growth lines. ICES J Mar Sci 50(4): 493-500

Rodland DL, Schöne BR, Helema S, Nielsen JK, Baier S (2006) A clockwork mollusc: ultradian rhythms in bivalve activity revealed by digital photography. J Exp Mar Bio Ecol 334: 316–323

734 Ropert M, Pien S, Mary C, Bouchaud B (2007) Rapport REMONOR, Résultats 2006, Ifremer,
735 70 pp
736 Salvi D, Mariottini P (2017) Molecular taxonomy in 2D: a novel ITS2 rRNA sequence-
737 structure approach guides the description of the oysters' subfamily Saccostreinae and
738 the genus *Magallana* (Bivalvia: Ostreidae). Zool J Linnean Soc 179: 263–276
739 Schöne BR (2008) The curse of physiology—challenges and opportunities in the
740 interpretation of geochemical data from mollusk shells. Geo-Mar Lett 28(5): 269-285
741 Schöne B (2013) *Arctica islandica* (Bivalvia): a unique paleoenvironmental archive of the
742 northern North Atlantic Ocean. Global Planet Change 111: 199–225
743 Schöne BR, Surge, D (eds) (2005) Looking back over skeletal diaries -high-resolution
744 environmental reconstructions from accretionary hard parts of aquatic organisms.
745 Palaeogeogr Palaeoclimatol Palaeoecol 228:1–191
746 Schöne BR, Giere O (2005) Growth increments and stable isotope variation in shells of the
747 deep-sea hydrothermal vent bivalve mollusk *Bathymodiolus brevior* from the North Fiji
748 Basin. Pacific Deep Sea Res Part 1 Oceanogr Res Pap 52(10): 1896-1910
749 Schöne BR, Lega J, Flessa KW, Goodwin DH, Dettman DL (2002a) Reconstructing daily
750 temperatures from growth rates of the intertidal bivalve mollusk *Chione cortezi*
751 (northern Gulf of California, Mexico). Palaeogeogr Palaeoclimatol Palaeoecol 184(1):
752 131-146
753 Schöne BR, Goodwin DH, Flessa KW, Dettman DL, Roopnarine PD (2002b)
754 Sclerochronology and growth of the bivalve molluscs *Chione* (*Chionista*) *fluctifraga*
755 and *Chione* (*Chionista*) *cortezi* in the northern Gulf of California, Mexico. The Veliger
756 45: 45–54
757 Schöne BR, Oschmann W, Rössler J, Freyre Castro AD, Houk SD, Kröncke I, Dreyer W,
758 Janssen R, Rumohr H, Dunca E (2003) North Atlantic oscillation dynamics recorded in

759 shells of a long-lived bivalve mollusk. Geology 31: 1237–1240
760 Scourse J, Richardson C, Forsythe G, Harris I, Heinemeier J, Fraser N, Briffa K, Jones P
761 (2006) First cross-matched floating chronology from the marine fossil record: data from
762 growth lines of the long-lived bivalve mollusc *Arctica islandica*. Holocene 16: 967–974
763 Schwartzmann C, Durrieu G, Sow M, Ciret P, Lazareth CE, Massabuau JC (2011) In situ
764 clam growth rate behavior in relation to temperature: a one-year coupled study of high-
765 frequency noninvasive valvometry and sclerochronology. Limnol Oceanogr 56: 1940–
766 1951
767 Soletchnik P, Geairon P, Razet D, Goulletquer P (1996) Physiologie de la maturation et de la
768 ponte chez l'huître creuse *Crassostrea gigas*. Rapport Ifremer, pp. 2-34
769 Surge D, Lohmann KC (2008) Evaluating Mg/Ca ratios as a temperature proxy in the
770 estuarine oyster, *Crassostrea virginica*. J Geophys Res Biogeosci 113 (G2)
771 Surge D, Lohmann KC, Dettman DL (2001) Controls on isotopic chemistry of the American
772 oyster, *Crassostrea virginica*: implications for growth patterns. Palaeogeogr
773 Palaeoclimatol Palaeoecol 172: 283–296
774 Thomson DJ (1982) Spectrum estimation and harmonic analysis. Proc IEEE 70(9): 1055-
775 1096
776 Tran D, Nadau A, Durrieu G, Ciret P, Parisot JP, Massabuau JC (2011) Field chronobiology
777 of a molluscan bivalve: how the moon and sun cycles interact to drive oyster activity
778 rhythms. Chronobiol int 28(4): 307-317
779 Tynan S, Dutton A, Eggins S, Opdyke B (2014) Oxygen isotope records of the Australian flat
780 oyster (*Ostrea angasi*) as a potential temperature archive. Mar Geol 357 195–209
781 Tynan S, Opdyke BN, Walczak M, Eggins S, Dutton A (2017) Assessment of Mg/Ca in
782 *Saccostrea glomerata* (the Sydney rock oyster) shell as a potential temperature record.
783 Palaeogeogr Palaeoclimatol Palaeoecol 484 : 79–88

784 Ullmann CV, Wiechert U, Korte C (2010) Oxygen isotope fluctuations in a modern North Sea
785 oyster (*Crassostrea gigas*) compared with annual variations in seawater temperature:
786 Implications for palaeoclimate studies. Chem Geol 277(1): 160-166
787

787 **Figure Captions**

788

789 **Figure 1:** A: Location of the Arcachon basin where the juvenile oysters were recruited and of
790 the breeding site (red rectangle) in Normandy, northwestern France. B: Aerial photo of the
791 Baie des Veys (BDV) and geographic location of the breeding site. C: Illustration of the
792 disposition of the tables and pockets where oysters were bred. D: Detail of figure 1C.

793

794 **Figure 2:** Variations of the environmental parameters during 2005 and 2006, directly
795 measured above the oyster tables. Temperature and salinity were measured every 15 mn.
796 Chlorophyll *a* and pheopigment concentrations were measured fortnightly. The elevation of
797 the water level above or below the oyster tables is reported for each high and low tide, as well
798 as the daily emersion duration. The dotted line represents the top of the oyster tables.

799

800 **Figure 3:** Observation of the section of an oyster hinge (sample BDV5) under
801 cathodoluminescence (CL). A: Thick section of the whole hinge of the oyster. B: Detail of
802 part of the hinge observed under CL and the associated luminescence profile. Seventy nine
803 increments were counted in 44 days and 77 in the following 43 days. The dotted white line
804 shows the analyzed profile. C: Example of revelation of the chemical markings (high
805 luminescence highlighted by the date of staining). Detail of the CL image illustrating the
806 alternating bright and dull bands. The white arrows show one CL increment as the distance
807 between two successive bright intervals.

808

809 **Figure 4:** Size-at-age and Von Bertalanffy growth model estimated for *Magallana gigas* at
810 the Baie des Veys (Normandy, France) based on 11 oyster hinge analyzes. Growth is fast
811 during the first year of life and then decreases through time. A significant variability is

812 observed between the 11 shells and could be related to inter-specific variability. Black dots
813 show the date of the 15 chemical markings and the date of death are reported. The hinge
814 length refers to the length measured in the Baie des Veys, after transplantation from the
815 Arcachon Basin.
816
817 **Figure 5:** Variations of the mean growth rate and mean daily temperature calculated for the
818 intervals between successive Mn^{2+} markings in the Baie des Veys during 2005 and 2006. The
819 growth rate of the oysters was determined from measurements on cathodoluminescence
820 images of the hinge between two consecutive chemical markings. The vertical bars
821 correspond to the standard deviation of the growth rate determined from the measurements on
822 11 individuals.
823
824 **Figure 6:** Determination of the relationships between temperature and growth rate and
825 chlorophyll *a* and growth rate of oysters. The black dot represents the growth peak of
826 February 2005 and is not considered in the correlation. Correlations were tested using
827 Spearman coefficients.
828
829 **Figure 7:** CL increment width changes in the hinge of two *M. gigas* shells for samples BDV3
830 and BDV5. The mean number of increments formed per day between two successive
831 markings was calculated.
832
833 **Figure 8:** The staining of 02/09/05 appears twice, which corresponds to increment formation
834 in less than 4 hours.
835

836 **Figure 9:** Correlation between increment widths and sea surface temperature for periods
837 when ~2 increments per day are mineralized in 2005 and in 2006 for A: sample BDV 3 and B:
838 sample BDV5. Note that the scale of the high tide level is inverted for a better visualization of
839 the correlation with increment width fluctuations.
840
841 **Figure 10:** Principal component analysis for samples BDV3 and BDV5 during the intervals
842 when ~2 increments are mineralized per day. We tested the relationship between the
843 increment width and mean daily temperature, salinity, immersion duration, high tide level and
844 low tide level.
845
846 **Figure 11:** Correlation between the number of increments and the length of carbonate
847 mineralized in the hinge area between the markings of 02/09/05 and 02/24/05.
848
849 **Table 1:** Number of CL increments counted between consecutive chemical markings and
850 determination of the mean number of increments mineralized per day for each interval.
851
852
853

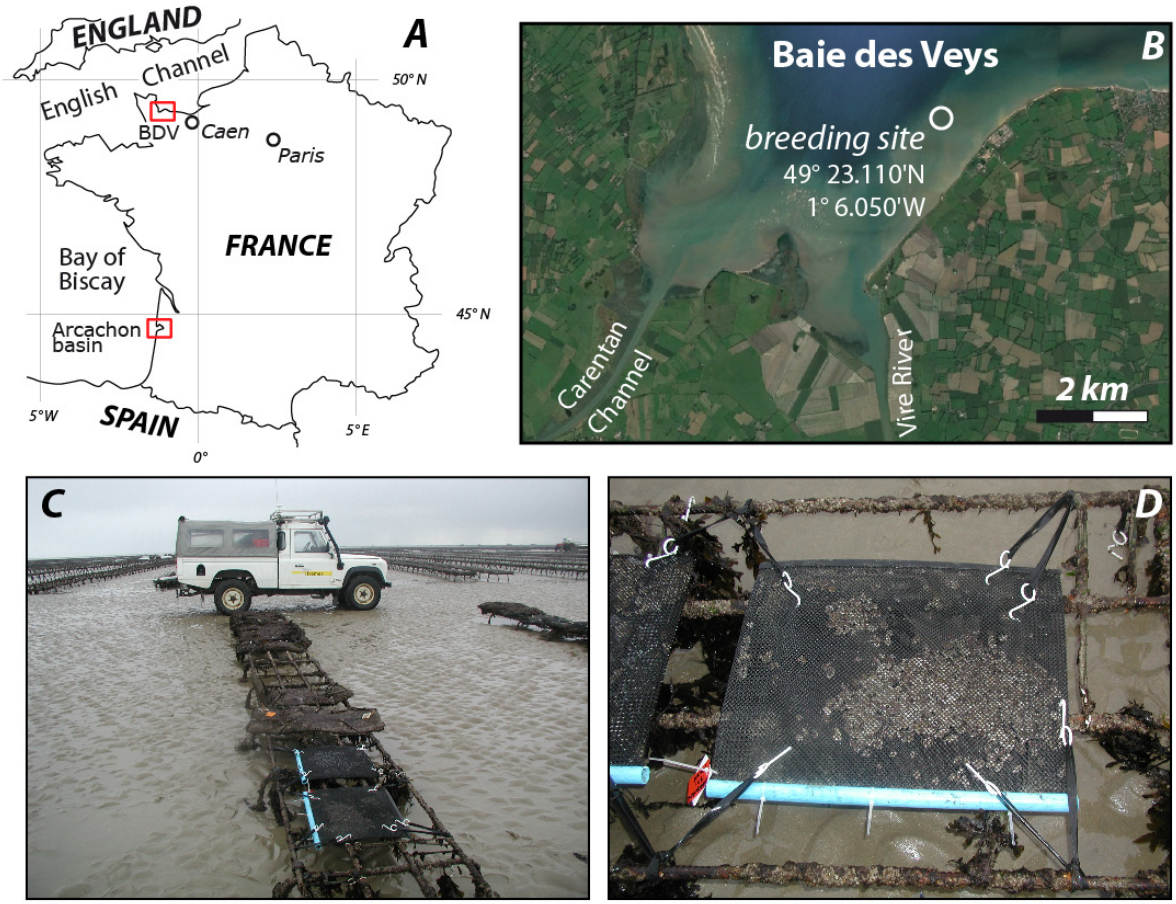

Figure 1

853
854
855

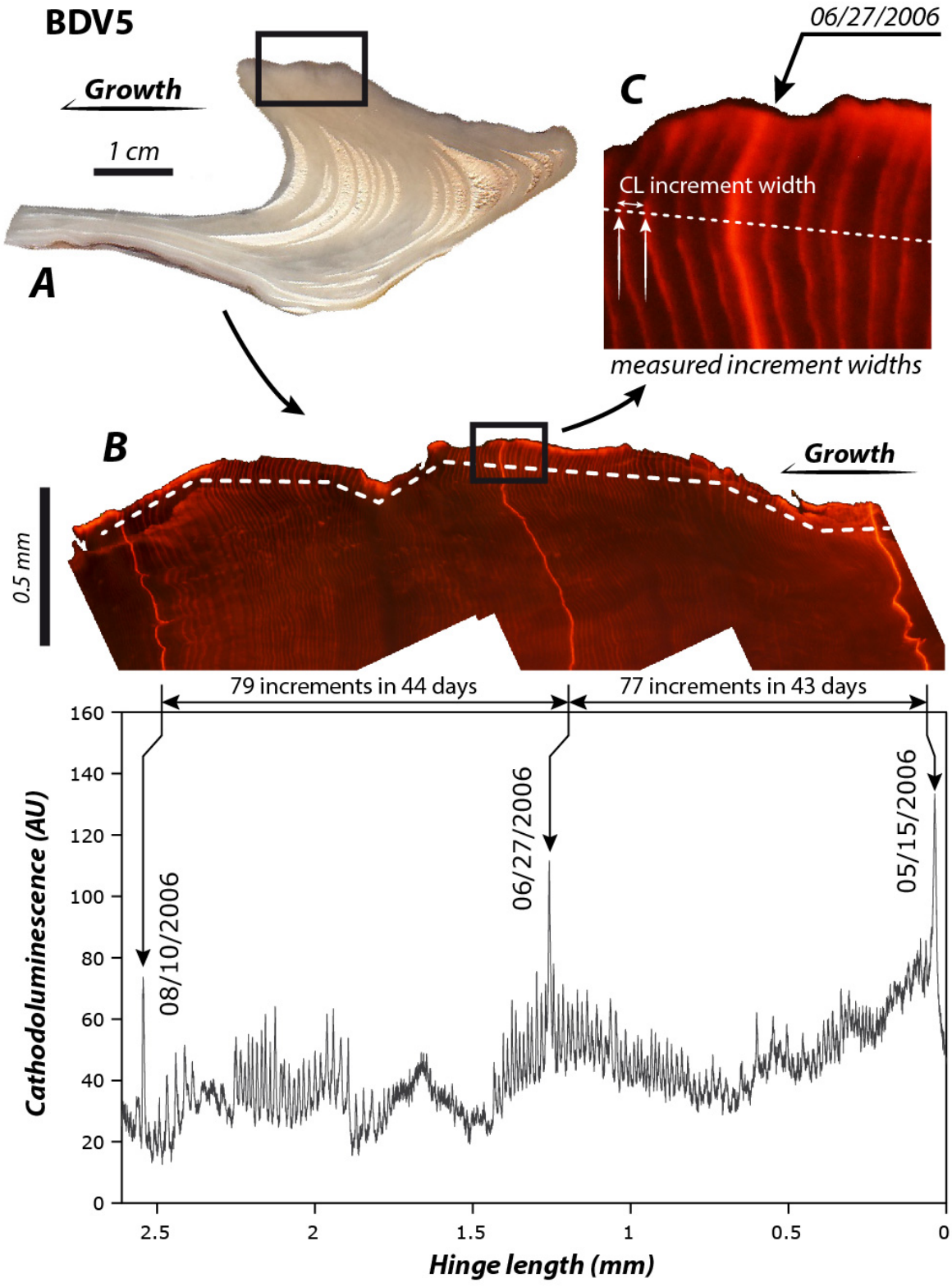

Figure 2

856
857

858

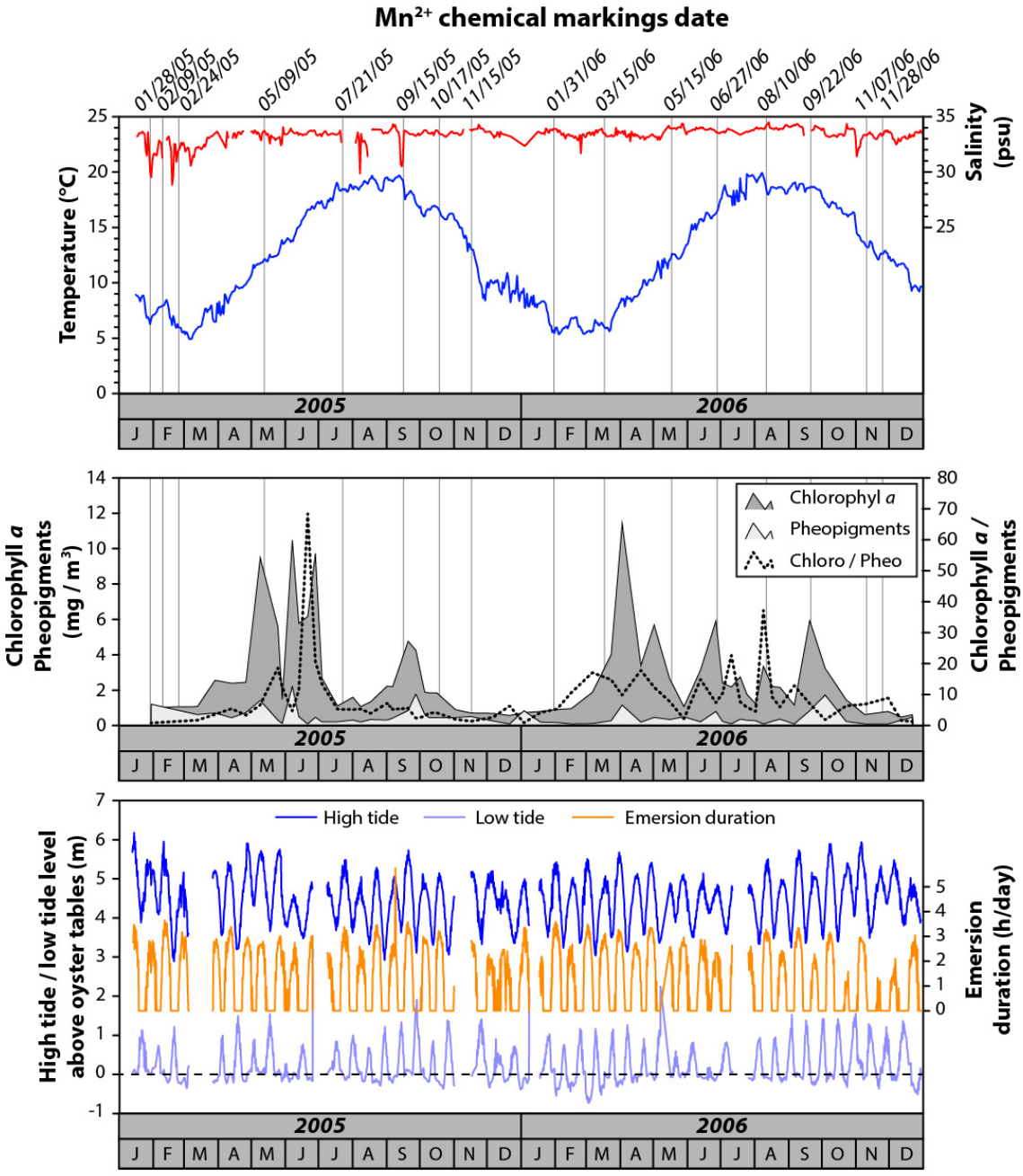

Figure 3

859
860
861

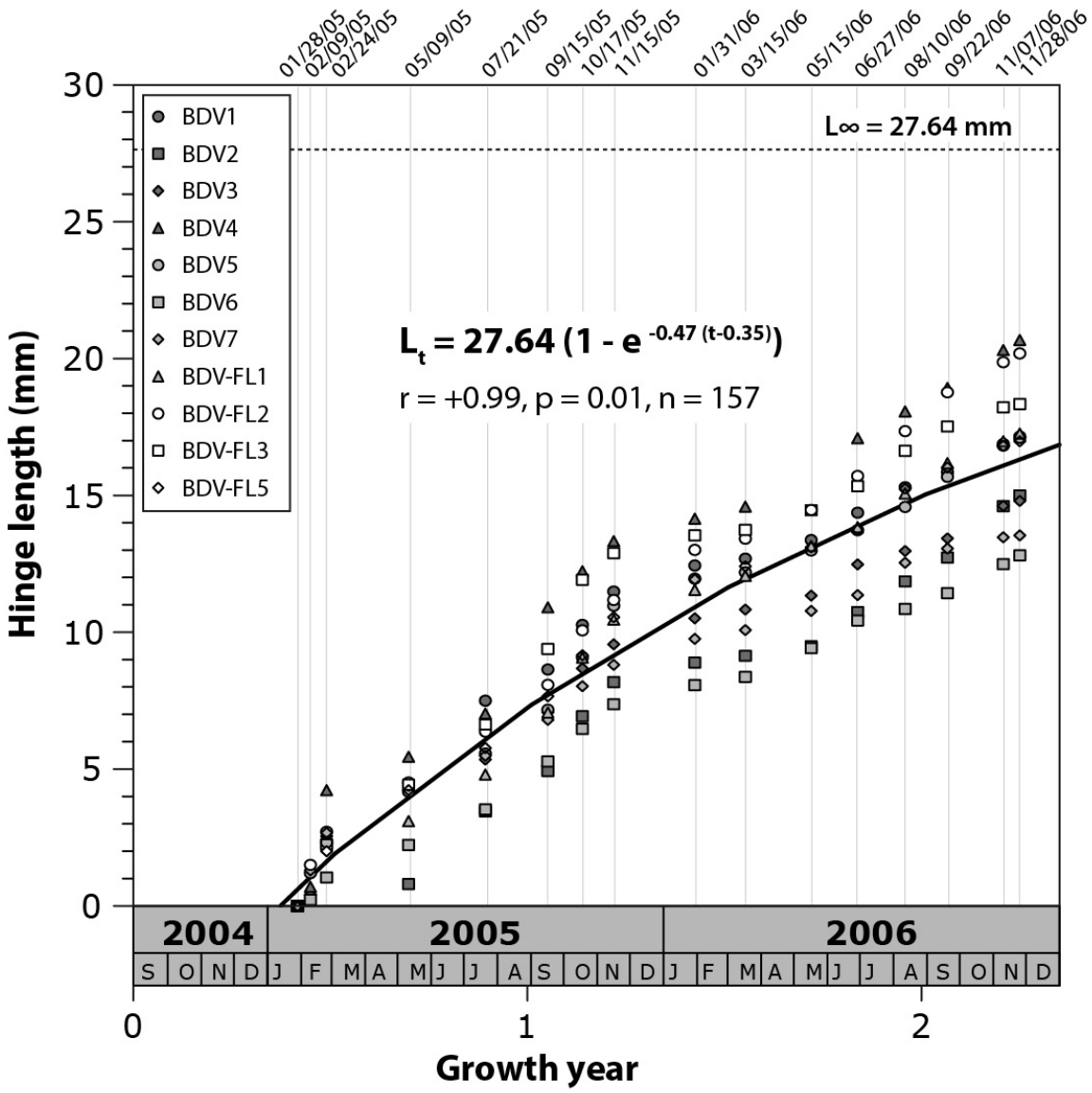
01/28/05
02/09/05
02/24/05
05/09/05
07/21/05
09/15/05
10/17/05
11/15/05
01/31/06
03/15/06
05/15/06
06/27/06
08/10/06
09/22/06
11/07/06
11/28/06
BDV1
BDV2
BDV3
BDV4
BDV5
BDV6
BDV7
BDV-FL1
BDV-FL2
BDV-FL3
BDV-FL5
L∞ = 27.64 mm
$L_t = 27.64 (1 - e^{-0.47 (t-0.35)})$
r = +0.99, p = 0.01, n = 157
Hinge length (mm)
Growth year
2004
2005
2006
S O N D J F M A M J J A S O N D J F M A M J J A S O N D

Figure 4

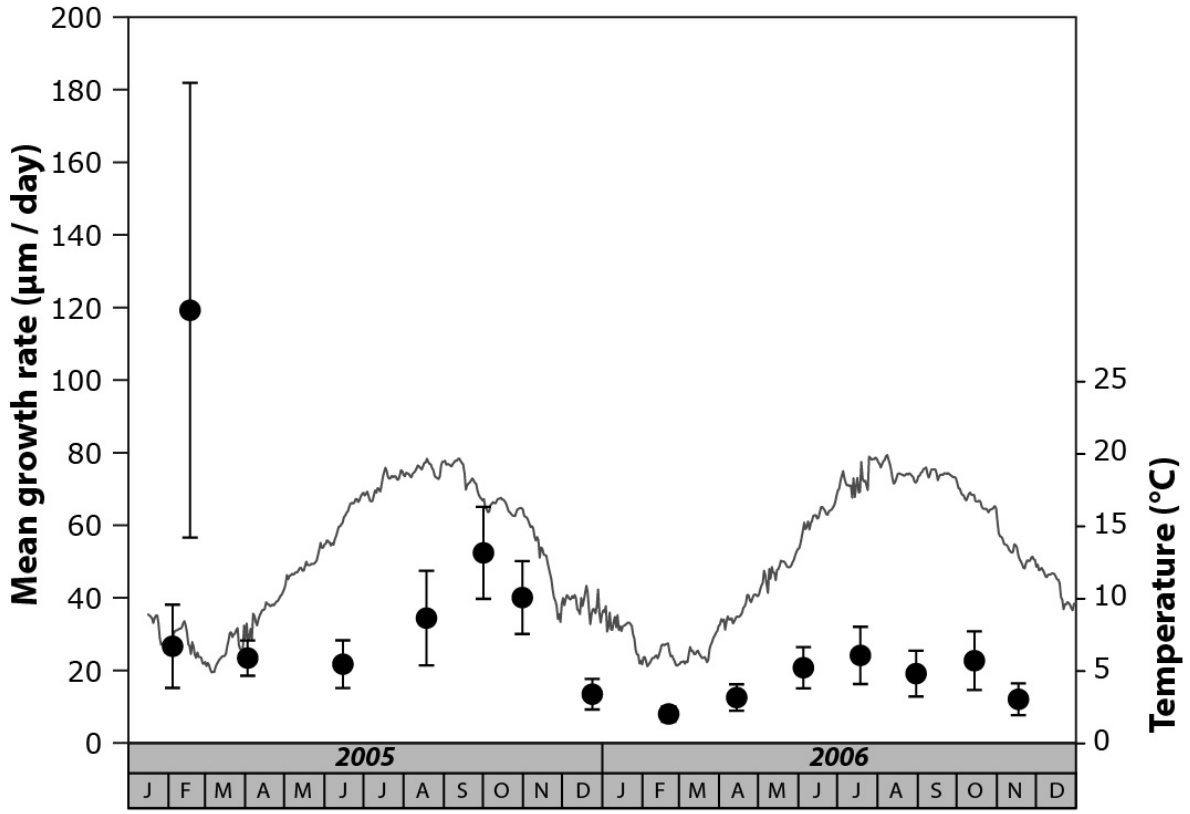
Mean growth rate (µm / day)
Temperature (°C)
200
180
160
140
120
100
80
60
40
20
0
25
20
15
10
5
0
2005
2006
J F M A M J J A S O N D J F M A M J J A S O N D

Figure 5

875

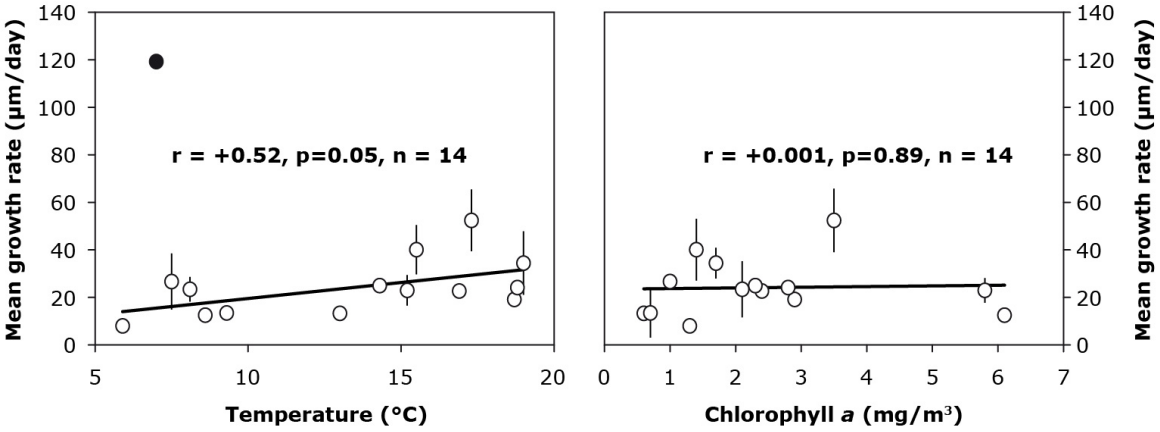

Figure 6

876
877

877

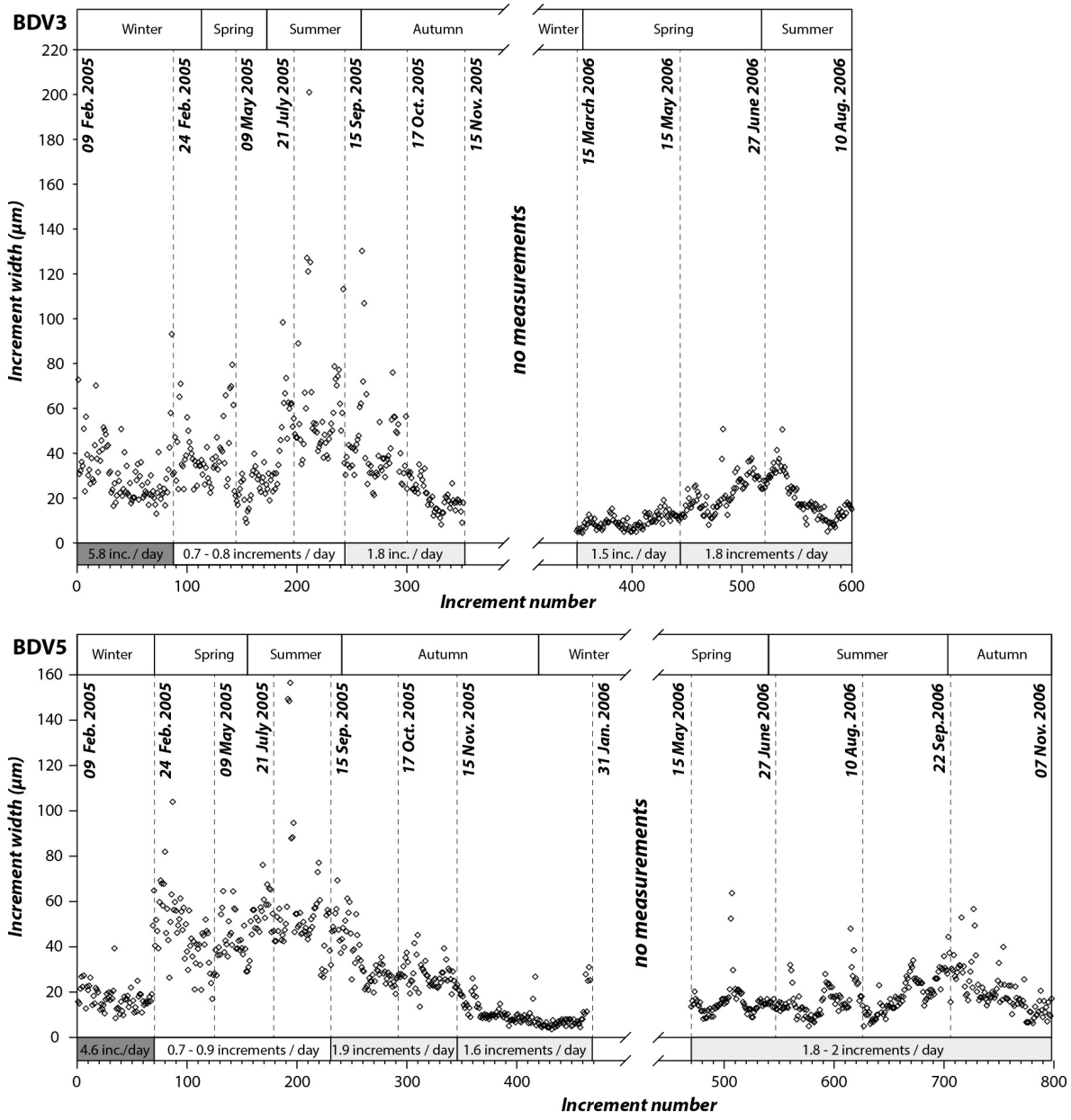

Figure 7

878
879
880
881
882

882

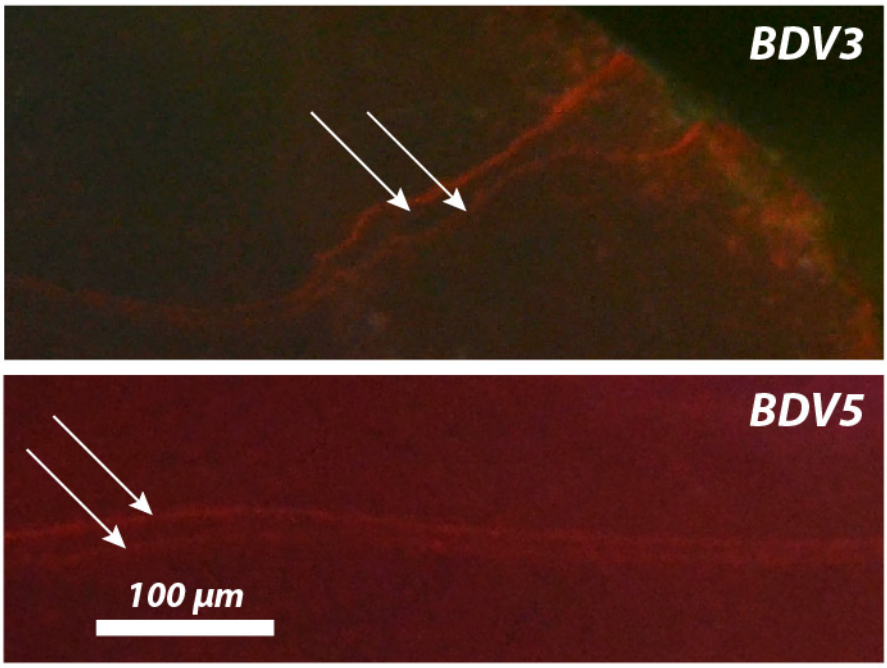

Figure 8

883
884
885
886
887

887

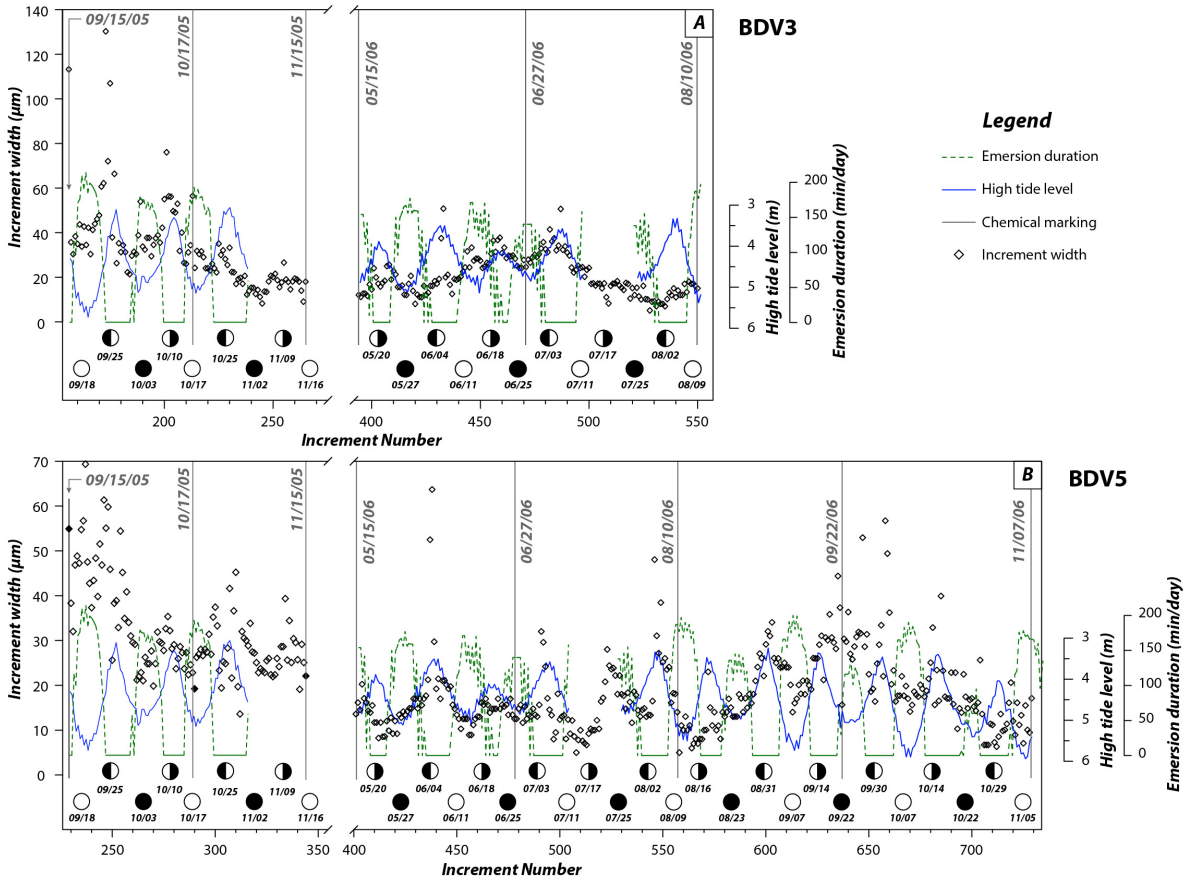

888
889
890
891

Figure 9

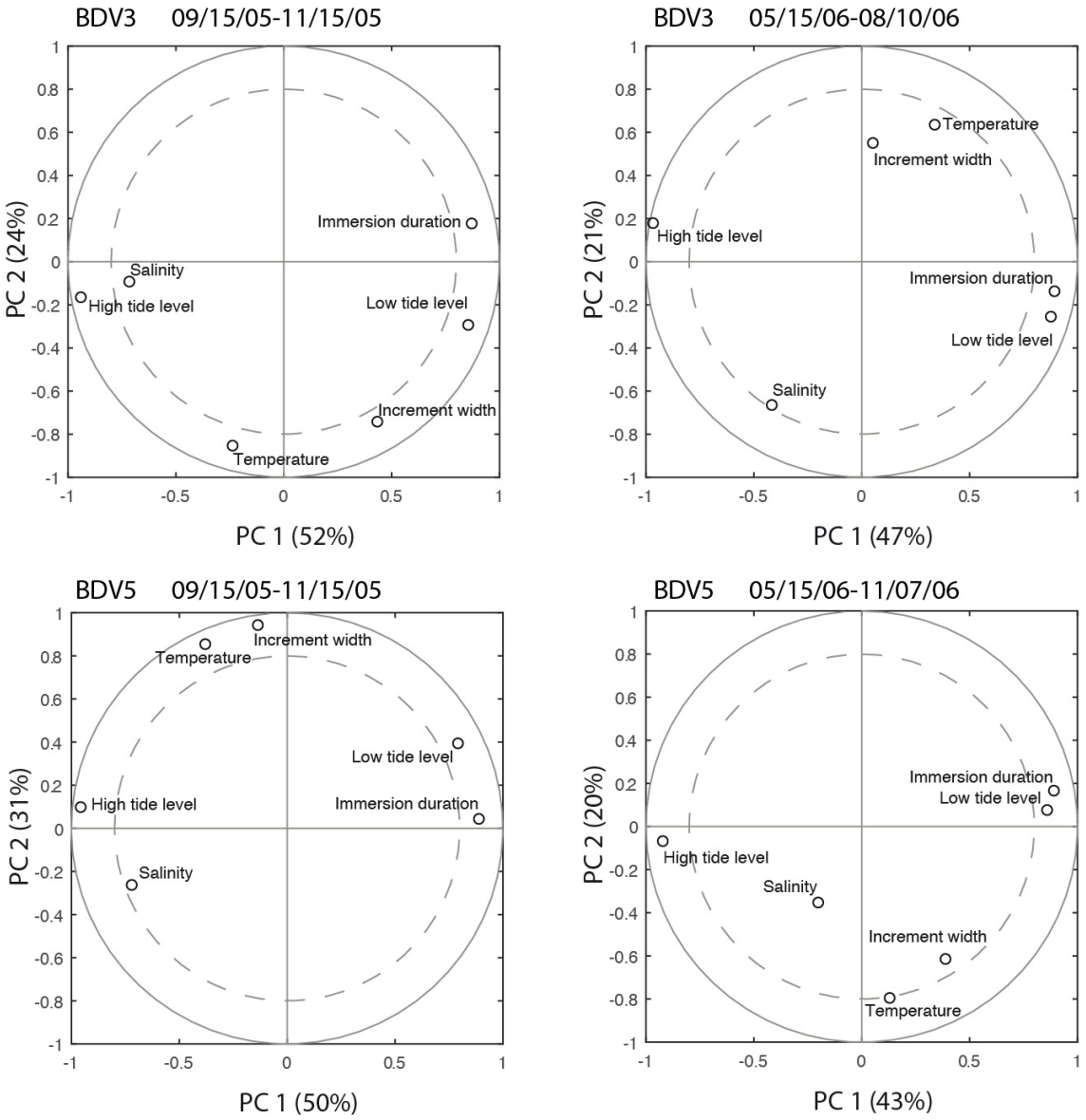
BDV3 09/15/05-11/15/05
Immersion duration
Salinity
High tide level
Low tide level
Increment width
Temperature
PC 2 (24%)
PC 1 (52%)
BDV3 05/15/06-08/10/06
Temperature
Increment width
High tide level
Immersion duration
Low tide level
Salinity
PC 2 (21%)
PC 1 (47%)
BDV5 09/15/05-11/15/05
Increment width
Temperature
Low tide level
High tide level
Immersion duration
Salinity
PC 2 (31%)
PC 1 (50%)
BDV5 05/15/06-11/07/06
Immersion duration
Low tide level
High tide level
Salinity
Increment width
Temperature
PC 2 (20%)
PC 1 (43%)

Figure 10

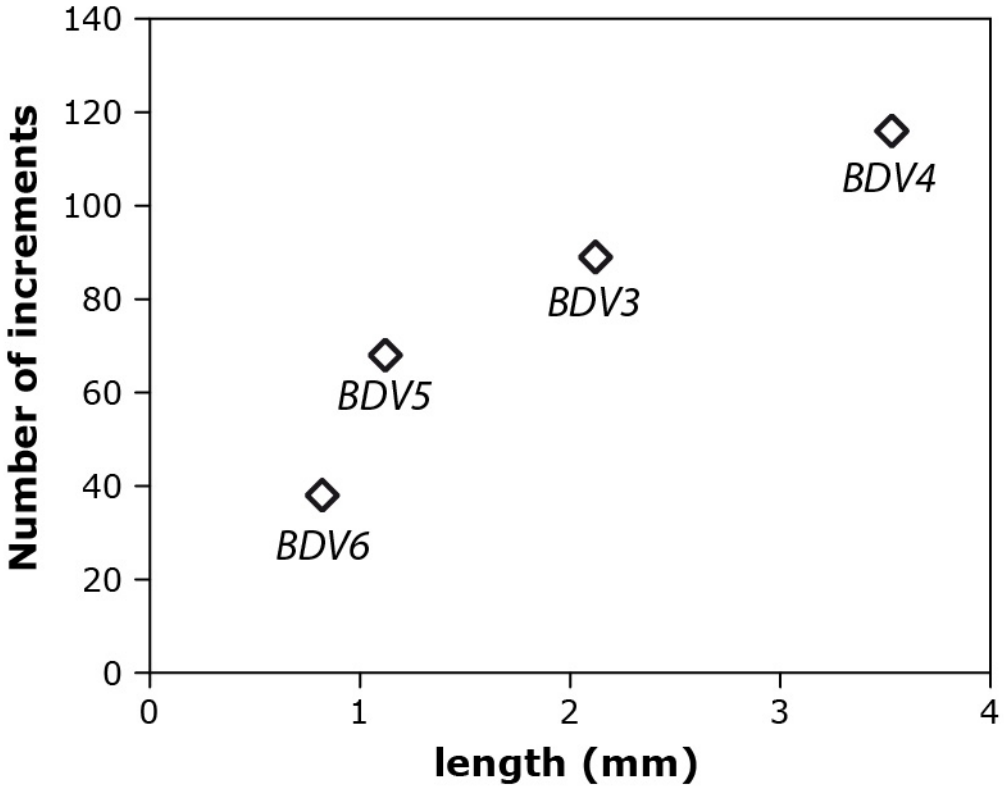
Number of increments
length (mm)
BDV4
BDV3
BDV5
BDV6
0
20
40
60
80
100
120
140
0
1
2
3
4

Figure 11

	02/09/05 02/24/05	02/24/05 05/09/05	05/09/05 07/21/05	07/21/05 09/15/05	09/15/05 10/17/05	10/17/05 11/15/05	11/15/05 01/31/06	03/15/06 05/15/06	05/15/06 06/27/06	06/27/06 08/10/06	08/10/06 09/22/06	09/22/06 11/07/06
BDV2	-	-	56	51	53	-	-	-	-	-	68	85
BDV3	89	56	53	46	57	52	-	94	77	79	-	-
BDV4	116	54	60	43	64	49	-	-	-	-	-	-
BDV5	68	54	54	52	61	54	123	-	77	79	80	92
BDV6	38	41	43	52	55	47	-	83	70	-	67	70
BDV-FL1	-	-	-	-	-	-	-	-	-	-	81	-
BDV-FL2	-	-	-	-	-	-	-	-	61	82	76	-
BDV-FL3	-	-	-	-	-	-	-	-	75	76	-	-
BDV-FL5	-	-	-	-	-	-	-	-	-	73	-	-
increment mean	77.75	51.25	53.2	48.8	58,0	50.5	123,0	88.5	72,0	77.8	74.4	82.33
standard deviation	32.9	6.8	6.3	4.1	4.5	3.1	-	7.8	6.8	3.4	6.6	11.2
number of days	15	74	73	56	32	29	77	61	43	44	43	46
increments / day	**5.2**	**0.7**	**0.7**	**0.9**	**1.8**	**1.7**	**1.6**	**1.4**	**1.7**	**1.8**	**1.7**	**1.8**
standard deviation	2.2	0.1	0.1	0.1	0.1	0.1	-	0.1	0.2	0.1	0.2	0.2